Paper No.
06594

CORROSION NACExpo 2006
61ST ANNUAL CONFERENCE & EXPOSITION

EROSION CORROSION AND SYNERGISTIC EFFECTS IN DISTURBED LIQUID-PARTICLE FLOW

Ramakrishna Malka, Srdjan Nešić, and Daniel A. Gulino

Institute for Corrosion and Multiphase Technology
342 West State Street
Ohio University
Athens, OH 45701
USA

ABSTRACT

The present study has been conducted to investigate the interaction between corrosion and erosion processes and to quantify the synergism in realistic flow environments, including sudden pipe constrictions, sudden pipe expansions, and protrusions. Tests were conducted on AISI 1018 carbon steel using 1% wt sodium chloride (NaCl) solution purged with CO_2 as the corrosive media and silica sand as the erodent.

The experiments were designed to understand whether erosion enhances corrosion or corrosion enhances erosion and to evaluate the contribution of the individual processes to the net synergism. It was observed that erosion enhances corrosion and corrosion enhances erosion, with each contributing to significant synergism; however, the dominant process was the effect of corrosion on erosion.

Keywords: erosion, corrosion, flow loop, steel LPR

INTRODUCTION

Corrosion is a material degradation process which occurs due to chemical or electrochemical action, while erosion is a mechanical wear process.[1] When these two processes act together the conjoint action of erosion and corrosion in aqueous environments is known as erosion-corrosion. In oil and gas production systems erosion-

corrosion due to sand is an increasingly significant problem[2,3]. The combined effects of erosion and corrosion can be significantly higher than the sum of the effects of the processes acting separately.[1,4,5] This net effect is called synergism. As proposed by many researchers, this net effect is due to the enhancement of corrosion by erosion and/or enhancement of erosion by corrosion. [4,5]

Synergism was not well quantified or clearly understood in the past because of the lack of detailed knowledge of the separate kinetics of pure erosion and pure corrosion.[6] There are very few studies in which synergism was quantified;[6-10] however, most of the work was carried out using jet impingement apparatus or rotating cylinder electrode systems in which the flow patterns or hydrodynamics are very different from reality[11] making it difficult to transfer the results to large scale pipeline systems. Very little work was done using more realistic systems such as flow loops.[12,13,14] Therefore it was not possible to clearly separate the damage due to erosion and corrosion in a combined erosion-corrosion process, and hence it is still unclear whether corrosion enhancement due to erosion or erosion enhancement due to corrosion, if either, is dominant.

There has been extensive work done in understanding the pure corrosion and pure erosion mechanisms;[15-19] however, very little knowledge exists in understanding erosion-corrosion mechanisms. It is accepted that impinging particles remove deposits or the protective layer on the metal surface resulting in continuous exposure of fresh metal surface to the corrosive environment resulting in higher corrosion rates. Zhou, et al.[6] proposed that erosion affects corrosion by removal of surface deposits, increase of local turbulence, and surface roughening and that corrosion has little or no effect on erosion. On the other hand it was observed by some researchers that corrosion increases erosion.[20,22,23] Postlethwaite et al.[20] proposed that the effect of corrosion is to roughen the metal surface which in turn increases the erosion rate because the latter is very sensitive to the impact angle of the solid particles. This was seen even when the corrosion rate accounted for less than 10% of the total wear. Matsumura, et al. [21] suggested that erosion can be enhanced by corrosion through the elimination of the work-hardened layer. Burstein, et al. [22] proposed that the effect of corrosion on slurry erosion is mainly through detachment of the flakes formed by repeated impacts of solid particles.

Despite the extensive work done in the past there has been no clear understanding of erosion-corrosion interactions under realistic flow conditions. Hence, the aim of this work was to study erosion-corrosion due to sand and CO_2 in a recirculating flow loop. In

order to achieve the research objectives, a unique test flow loop was designed and developed with the aim to:

1. Investigate the erosion and corrosion interactions in realistic disturbed pipe flow conditions.

2. Perform in-situ, localized, electrochemical measurements as well as weight loss measurements to be able to separate the material loss due to the individual erosion and corrosion processes and to determine the major mechanism influencing the synergism.

EXPERIMENTAL

The experiments were done in a large scale (2000 liter) 4-inch flow loop to simulate real field conditions. Figure 1 shows a diagram of the loop which consists of a large stainless steel conical bottom tank from which the liquid solution (with or without sand) was drawn using a calibrated positive displacement pump. This pump circulates the liquid or the slurry through a 30-foot long, 4-inch ID PVC pipe connected to the bottom of the tank. Pump suction creates high turbulence inside the tank sufficient to keep the sand particles suspended. An erosion-corrosion test section was installed far downstream with isolation valves before and after, which helped with installation and removal of the test section without contaminating the test fluid with oxygen. The loop was connected to nitrogen (N_2) and carbon dioxide (CO_2) sources which were used for deoxygenation and saturation of the test fluid with CO_2 or N_2. A thermocouple was installed near the test section for temperature measurement. Sand could be sampled by using an adjustable sampling port near the test section.

Test Section Design

The test section, shown in Figure 2-Figure 6, enabled simultaneous study of erosion-corrosion across three different flow geometries that commonly occur in pipeline designs: a sudden pipe constriction, a sudden pipe expansion, and a protrusion. The test section consisted of a 4-inch ID pipe contracting into a 2.47-inch ID pipe and then expanding back into a 4-inch ID pipe (see Figure 2-Figure 3). This gives a diameter ratio of 1.61 and an area ratio of 2.6 for larger to smaller pipe cross sections. In the constricted section, a $\frac{1}{8}$-inch protrusion was installed in the form of a orifice (see Figure 4). The total length of the test section is 54 inches.

The test cell is segmented in order to enable local electrochemical and weight loss measurements across the flow disturbances. The ring-like specimens, made of the desired metal to be tested, slide into an outer tube made of acrylic, which was chosen because of its transparence and electrical insulation properties.

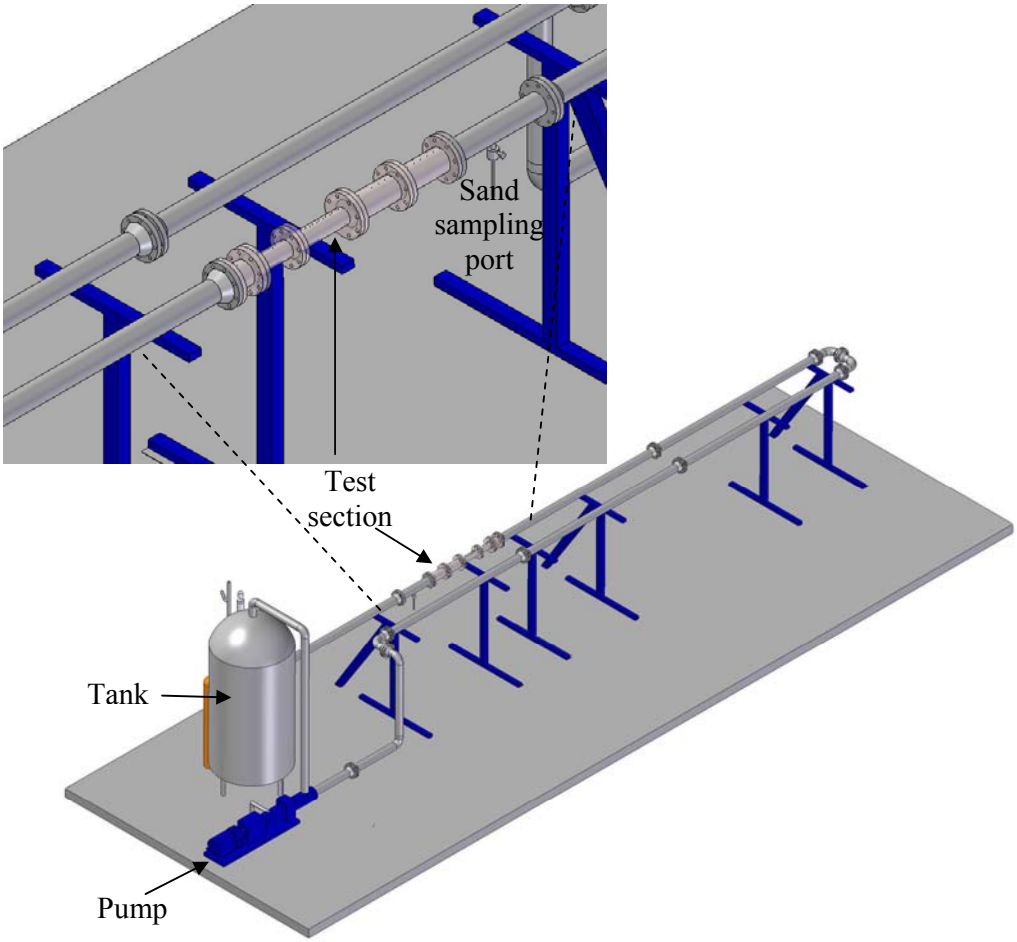

Figure 1. Diagram of the experimental flow loop with an enlarged view of the test section.

The specimens are electrically separated using O-rings made of Buna-N, which was selected because of its excellent compression properties, high electrical resistance, and resistance to oxidation and impact/abrasion. With the help of the outer acrylic tubing and the O-rings, it was possible to hold the specimens in compression, and hence good mechanical sealing was achieved. Electrical contact with the individual specimen was made using 10-32 stainless steel screws which passed through the outer acrylic tube with the help of 10-32 helical inserts embedded in the tubing (Figure 6).

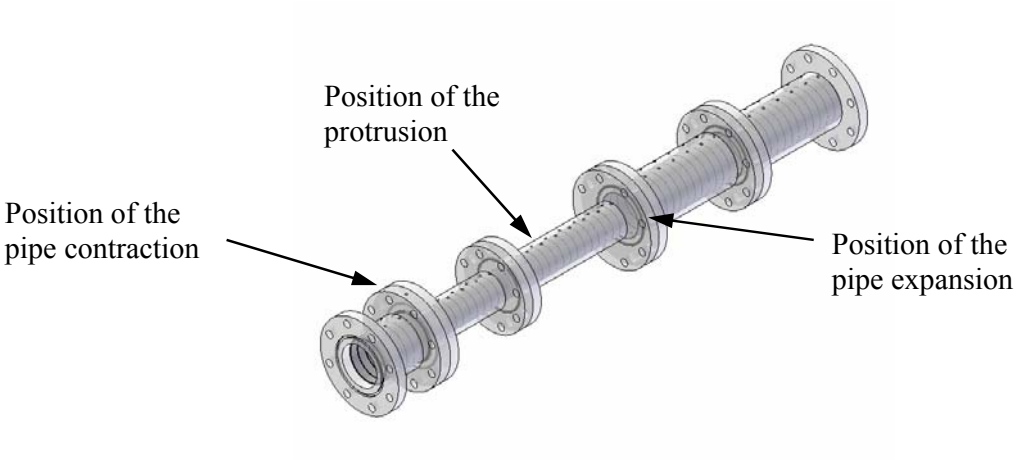

Figure 2. Isometric view of the test section.

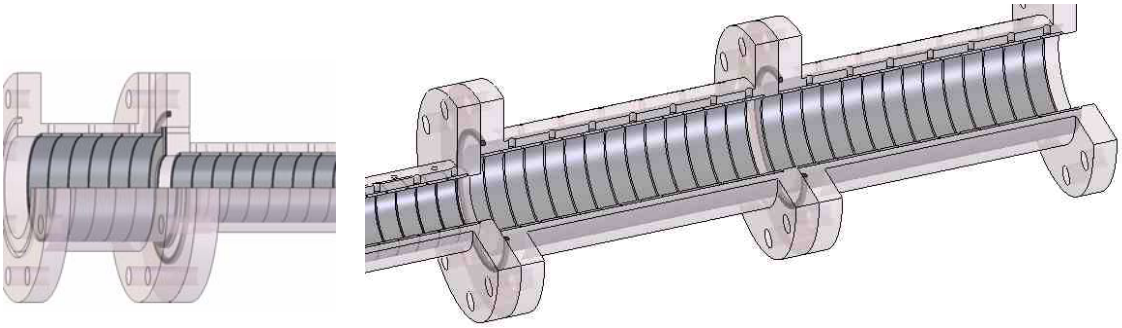

Figure 3. Sectional view of the test section showing the pipe constriction and expansion.

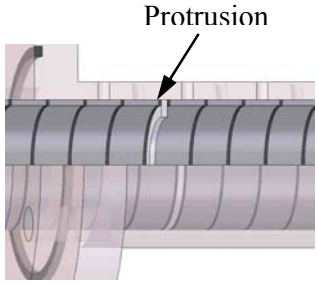

Figure 4. Sectional view of the test section showing the protrusion.

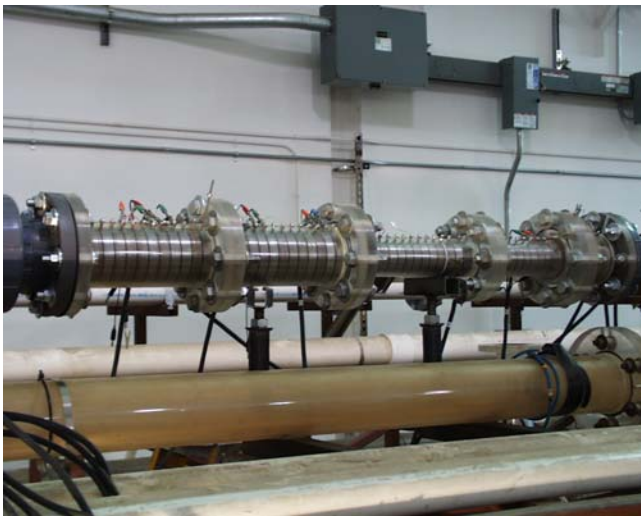

Figure 5. Photograph of the test section in place during the experiment.

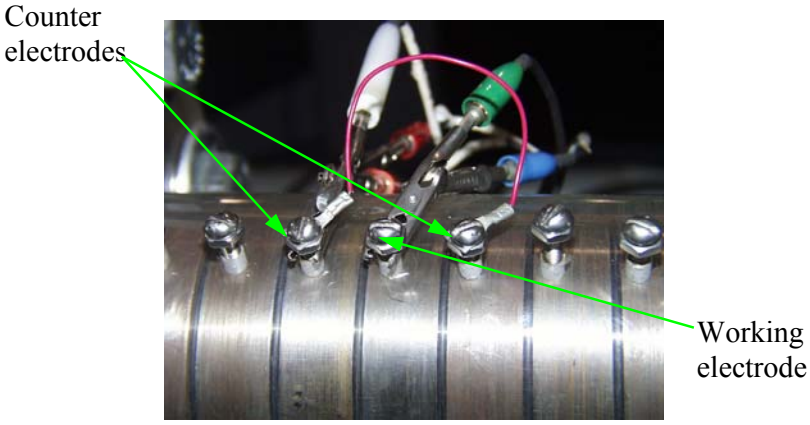

Figure 6. Enlarged photo showing electrical connections to the test section.

Test Matrix

With the aim of quantifying the synergism accurately, the test matrices shown in

Table I through Table III were followed. As this was only an initial study intended to investigate the basic erosion and corrosion interactions, the effect of such parameters as temperature, velocity, sand size, sharpness, and concentration, and pH, were outside of its scope. A liquid velocity of 2 m/s was selected to ensure that all sand particles were entrained. A pH value of 4.0 was selected to avoid any corrosion film formation.

Table I. Pure corrosion test matrix

Flow type	Single-phase: water
Temperature (^{o}C)	34
CO_2 partial pressure (bar)	1.2
Liquid velocity (m/s)	2
pH	4

Table II. Pure erosion test matrix

Flow type	Two-phase: water-sand
Temperature (^{o}C)	34
N_2 Partial pressure (bar)	1.2
Liquid velocity (m/s)	2
pH	7
Average sand size (micron)	275
Sand concentration (by weight)	2 %

Table III. Erosion-corrosion test matrix

Flow type	Two-phase: water-sand
Temperature (^{o} C)	34
CO_2 Partial pressure (bar)	1.2
Liquid velocity (m/s)	2
pH	4
Average sand size (micron)	275
Sand concentration (by weight)	2 %

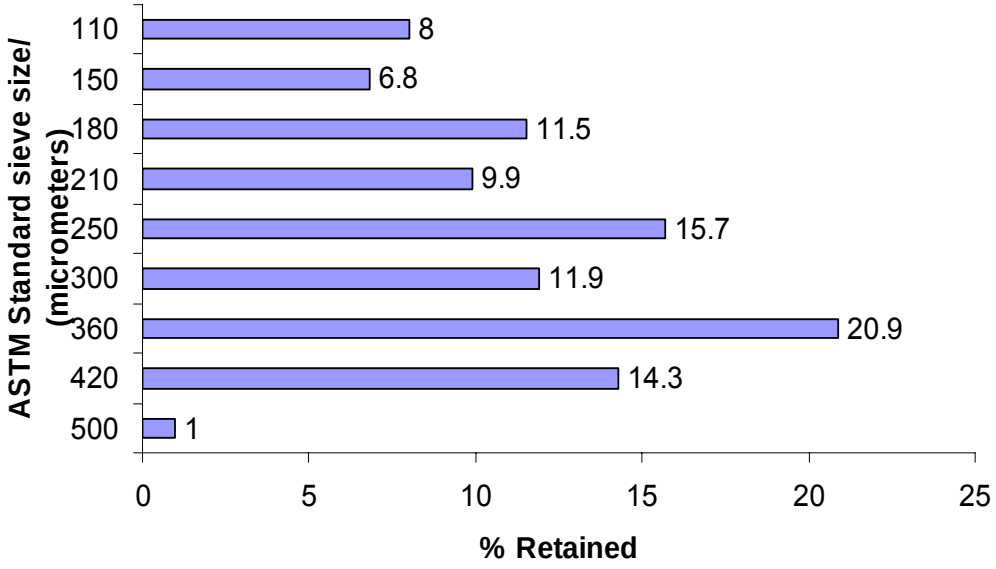

Figure 7. Size distribution of the silica sand particles used in the study.

Procedures

At the beginning of each experiment the tank and the flow loop with a dummy test section in place was filled with approximately 300 gallons of deionized water with 1% wt NaCl added. The solution was then purged with N_2 or CO_2 gas to saturate it and deoxygenate to below 20 ppb dissolved O_2. Heaters were used to maintain the desired temperature. The pH of the solution was adjusted from the equilibrium value to the desired value by adding a calculated amount of deoxygenated sodium bicarbonate solution. The test section was assembled (with the specimens previously polished with 400 grit sand paper and washed with alcohol), installed in place of the dummy cell and purged with N_2/CO_2 to avoid oxygen contamination. The length of the experimental runs was 4 to 24 hours. During the experiments, parameters such as pH, temperature, and pressure were regularly monitored and adjusted if needed.

The first, pure corrosion, series of experiments was conducted using 1% wt NaCl solution adjusted to pH 4 and saturated with carbon dioxide. Linear Polarization Resistance (LPR, two electrode procedure[22]) and weight loss (WL) techniques were used to measure the "pure" corrosion rate (CR_{PC}), i.e. the corrosion rate in the absence of erosion, for each specimen across the test section.

The second, "pure" erosion, series of experiments was conducted using 2% wt silica sand (size distribution is given in Figure 7) suspended in a 1% wt NaCl solution saturated with N_2 at pH 7. The neutral pH and N_2 were used to minimize any corrosion

during the experiments. The weight loss method was used for measuring the pure erosion rate (ER_{PE}).

The third and final series of erosion-corrosion experiments were conducted using the same 2% wt silica sand suspended in a 1% wt NaCl solution saturated with carbon dioxide adjusted to pH 4. In these experiments, the corrosion component (CR_{EC}) was obtained using the LPR technique which measured only the electrochemical component of the metal loss (metal loss due to corrosion only). The erosion component (ER_{EC}) was derived from the difference between the total weight loss (WL_{EC}) as measured by weight loss and the corrosion component (CR_{EC}) as explained below. Hence the increment in corrosion due to erosion, increment in erosion due to corrosion, and the total synergism were obtained as follows:

Pure corrosion rate:	CR_{PC} (measured)
Pure erosion rate:	ER_{PE} (measured)
Erosion-corrosion rate:	WL_{EC} (measured)
Corrosion rate component in erosion corrosion:	CR_{EC} (measured)
Erosion rate component in erosion corrosion:	$ER_{EC} = WL_{EC} - CR_{EC}$
Increment in erosion due to corrosion:	$\Delta ER = ER_{EC} - ER_{PE}$
Increment in corrosion due to erosion:	$\Delta CR = CR_{EC} - CR_{PC}$
Net synergism:	$\Delta Syn = \Delta CR + \Delta ER$

RESULTS

Pure corrosion experiments

The pure corrosion experiments were conducted for 24 hours, and typical results are shown in Figure 8. The corrosion rate obtained from the LPR method is the average of five data points taken within the span of experiment. The WL data shown are the average from the two separate runs. The overall agreement between the LPR and WL measurements is rather good given the error level inherent to each technique as indicted by the error bars which show the maximum and minimum values. The constriction and expansion of the flow did not lead to significant changes in the corrosion rate while the protrusion did. The corrosion rates in the smaller, 2.47-inch ID section were generally lower than the ones in the larger, 4-inch ID section. This was not as expected from theory because the Reynolds's number in the lower ID test section was 285,000, while in the larger it was 181,500. Therefore, higher turbulence and higher mass transfer rates were

expected in the lower ID section which should have resulted in higher corrosion rates at pH 4. This unexpected trend could possibly be attributed to subtle differences in metallurgy. The specimens used for the small and large ID sections were made from two different batches of nominally identical AISI 1018 steel. Even if both parent steels met the AISI 1018 specifications (see the composition in Table IV), it is assumed that unspecified metallurgical differences in the steels led to the reverse corrosion trend. For the purpose of further calculations, the pure corrosion rate, CR_{PC}, was considered to be the average of the LPR and weight loss data obtained.

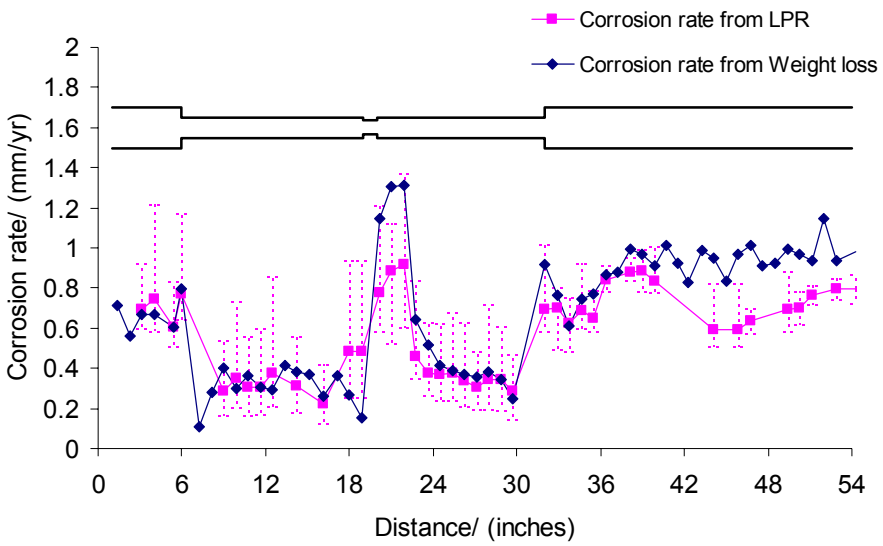

Figure 8. Pure corrosion rate across the flow disturbances (single phase flow, pH 4, P_{CO2} =1.2 bar, 24 hrs)

Table IV. Composition (per cent) of the AISI 1018 steel specimen.

Element	4” ID section specimen	constriction specimen	2.47” ID section specimen
Al	0.039	0.031	0.027
As	0.007	0.008	0.007
B	0.001	0.001	0.001
C	0.24	0.18	0.24
Ca	0.002	0.000	0.002
Co	0.007	0.005	0.007
Cr	0.026	0.036	0.011
Cu	0.009	0.004	0.024
Mn	0.73	0.72	0.78
Mo	0.012	0.013	0.014
Nb	0.011	0.011	0.011
Ni	0.016	0.017	0.014
P	0.011	0.014	0.011
Pb	0.008	0.008	0.009
S	0.001	0.006	<0.001
Sb	0.023	0.025	0.023
Si	0.022	0.22	0.18
Sn	0.001	0.001	< 0.001
Ta	< 0.001	< 0.001	< 0.001
Ti	< 0.001	< 0.001	< 0.001
V	0.001	< 0.001	< 0.001
Zr	0.003	0.003	0.003

Pure erosion experiments

The pure erosion experiment was conducted twice, and the results are shown in Figure 9. The duration of these tests was limited to 4 hours to minimize the effect of sand degradation with time. As expected, the erosion rate was significantly higher in the lower ID section where the velocity, Reynolds number, and turbulence levels were much higher. Contrary to expectations, the constriction and expansion did not lead to higher erosion rates; however, significant increases in erosion were seen downstream of the protrusion.

The low corrosion rate obtained with LPR measurements shown in Figure 9 is consistent with the absence of corrosive species in a N_2 purged solution at pH 7. Therefore, it was confirmed that in these experiments the contribution of corrosion to the total weight loss could be ignored.

Sand was sampled before and after for each experiment, and SEM (Scanning Electron Microscope) micrographs of the samples are shown in Figure 10. Those with

different magnifications show the sharpness of the particles as well as their surface roughness and confirm that the sand was not degraded significantly within the duration of the experiment.

The average pure erosion rate, ER_{PE}, along the test section used in subsequent calculations was obtained by averaging the weight loss data from the two experiments.

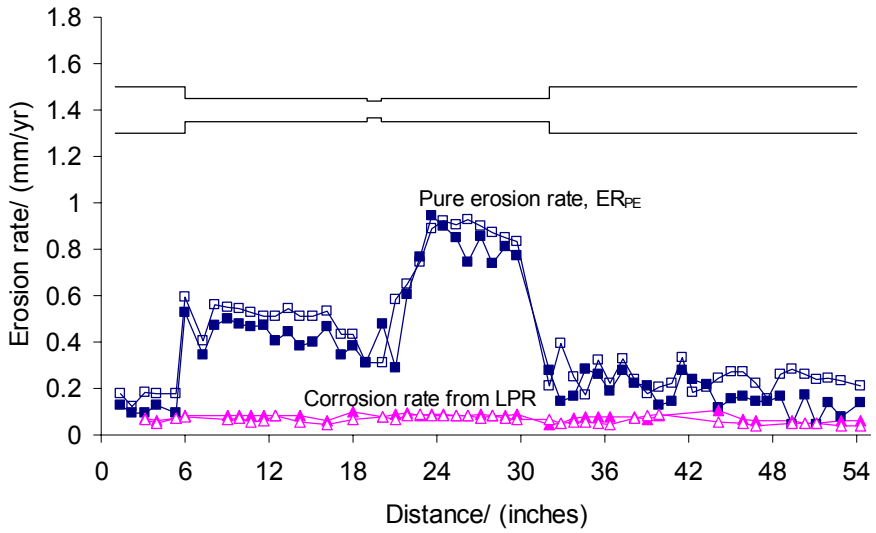

Figure 9. Pure erosion rate across the flow disturbances (2%wt sand slurry, pH 7, P_{N2}=1.2bar, 4 hrs, silica sand).

Before exposure

After exposure

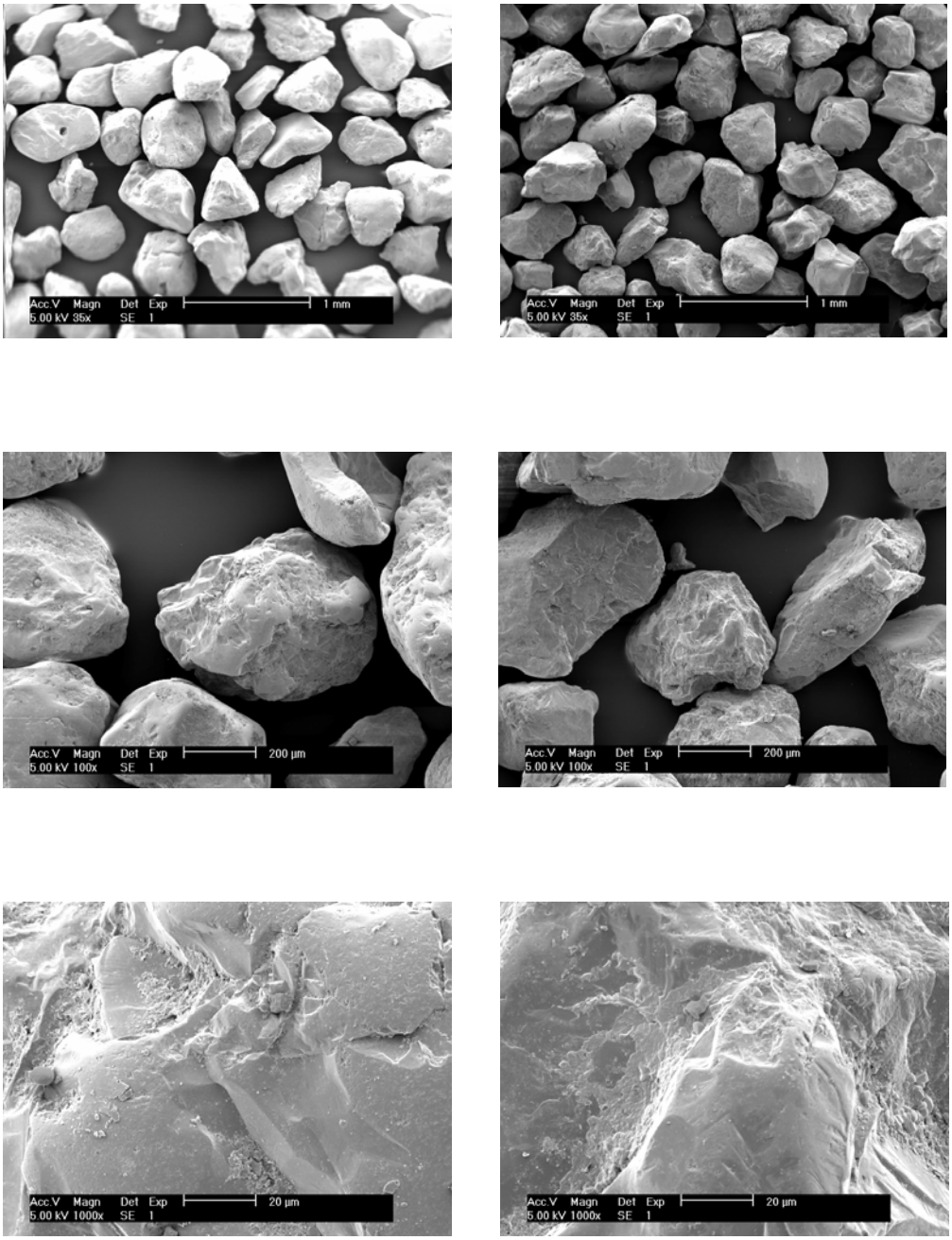

Figure 10. Sand particles at different magnifications before erosion (left column) and after being exposed for 4 hr in an erosion experiment (right column).

Erosion-corrosion experiments

The erosion-corrosion experiment was also conducted twice using silica sand and CO_2-saturated water. To minimize the effect of sand degradation the duration of these experiments was also limited to 4 hours. The tests were repeatable as shown in the Figure 11.

In this experiments the LPR measurements were used to detect the metal loss only due to corrosion (CR_{EC}), while the weight loss detected the total metal loss due to combined erosion-corrosion attack (WL_{EC}). Clearly the overall level of erosion-corrosion was significantly higher then corrosion alone. Sand was sampled before and after each experiment. SEM pictures of the samples, shown in Figure 12, indicate that sand did not degrade within the duration of the experiments.

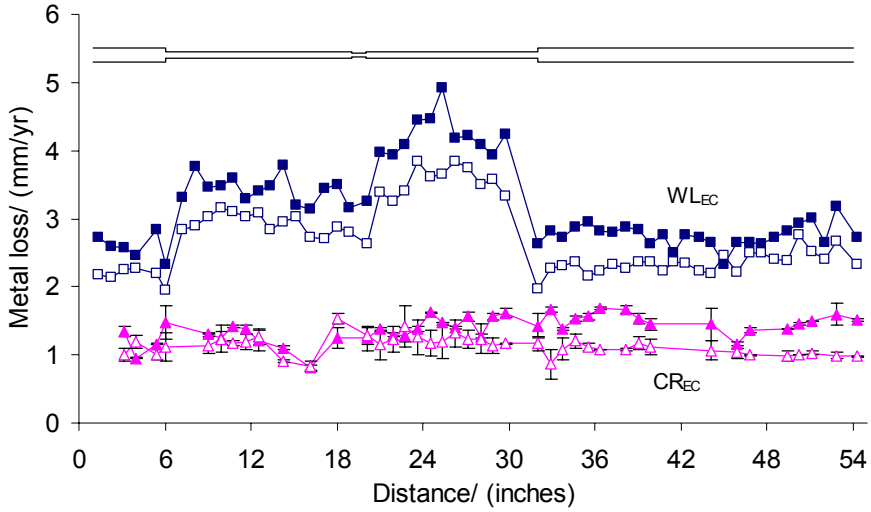

Figure 11. Metal loss across the flow disturbances in erosion-corrosion environment (2%wt sand slurry, pH 4, PCO2 1.2bar, 4 hrs, silica sand).

Before exposure

After exposure

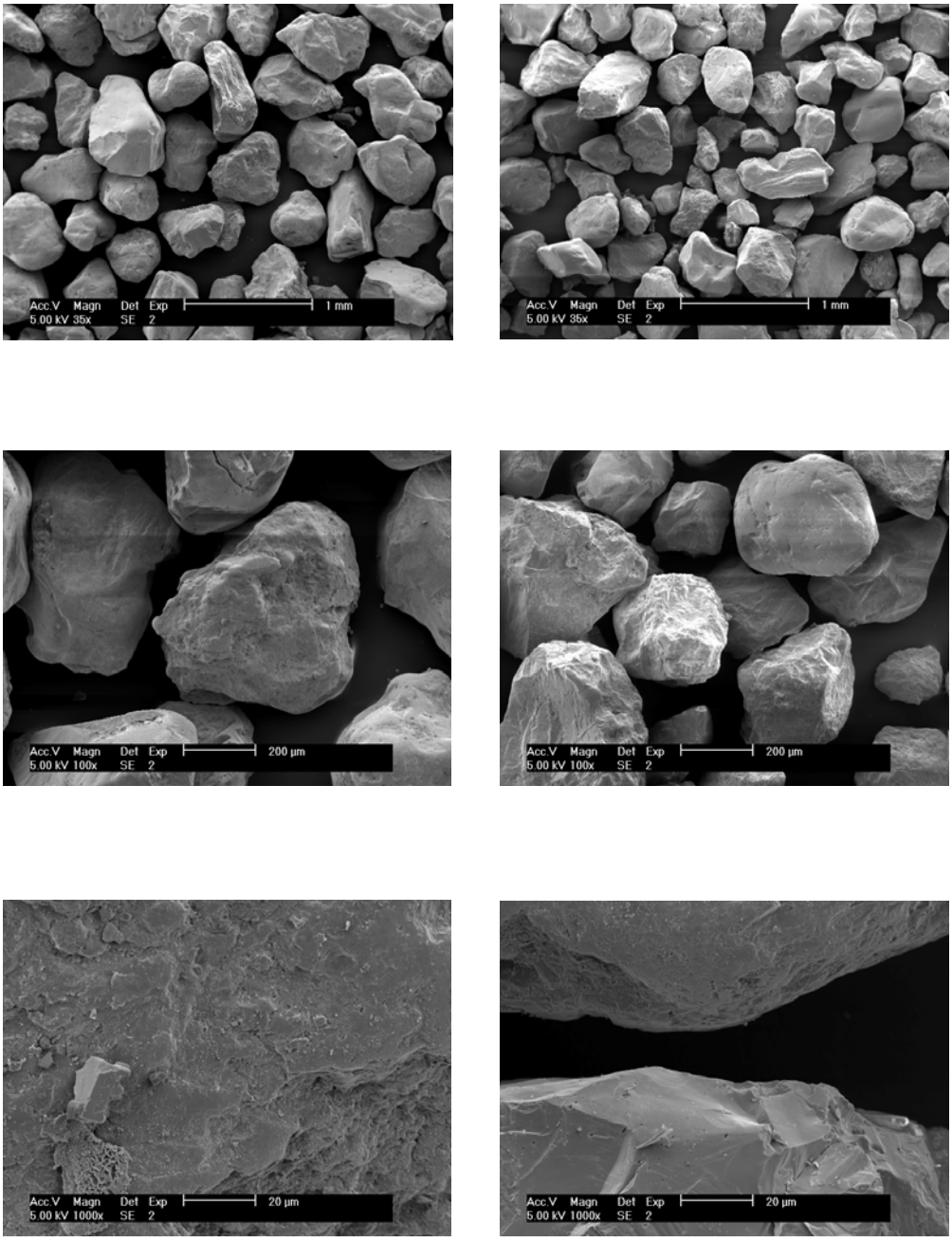

Figure 12. Sand particles at different magnifications before experiment (left column) and after being exposed for 4hr in an erosion-corrosion experiment (right column).

The total weight loss, WL_{EC}, used in subsequent calcuations is the average of weight loss values taken from the two erosion-corrosion experiments. The corrosion rate component in combined erosion-corrosion, CR_{EC}, was obtained from the average values of the LPR data taken from the two erosion-corrosion experiments.

Figure 13 shows the comparison between the metal loss due to pure corrosion, CR_{PC}, and the corrosion component in the erosion-corrosion experiment, CR_{EC}. It can be seen that there is a significant increase in the corrosion rate due to erosion along the entire test section. The average increment in corrosion rate due to erosion (ΔCR) was found to be up to twice that of the pure corrosion rate (CR_{PC}). Figure 14 shows the comparison of the pure erosion rate, ER_{PE}, and the erosion rate component in an erosion-corrosion experiment, ER_{EC}. A large increase in the erosion rate due to corrosion can be observed. The increment in erosion rate due to corrosion (ΔER) is found to be on average 3 to 4 times the pure erosion rate (ER_{PE}).

A comparison of the increment in erosion due to corrosion, ΔER, and the increment in corrosion due to erosion, ΔCR, is shown in Figure 15 and shows explicitly that the erosion rate is more affected by the synergism. The total synergism (ΔSyn) is shown in Figure 16 and is found to be approximately two times the total loss due to pure erosion and pure corrosion together ($ER_{PE} + CR_{PC}$). The contribution of ΔCR in ΔSyn was 30% while the contribution of ΔER was 70%.

DISCUSSION

From the results shown above, it can be concluded that due to the interactions of erosion and corrosion, both mechanisms of metal loss are enhanced by each other; however, the erosion enhancement due to corrosion is more significant. From Figure 13, it can be observed that corrosion is almost doubled in the presence of erosion. This observation supports previous speculation[4,5,6] that erosion affects corrosion by increase of local turbulence/mass transfer and by surface roughening.

In Figure 17(b) it can be observed that in pure erosion metal flakes are formed due to particle impacts. This supports the platelet mechanism proposed by Levy[18] which assumes that in erosion, plastic deformation occurs by repeated impacts resulting in deformation hardening of the surface flakes until they break off. In Figure 17(c) both effects of corrosion and erosion can be seen. It can be speculated that corrosion enhances erosion by accelerating the detachment of the flakes created by repeated particle impacts.

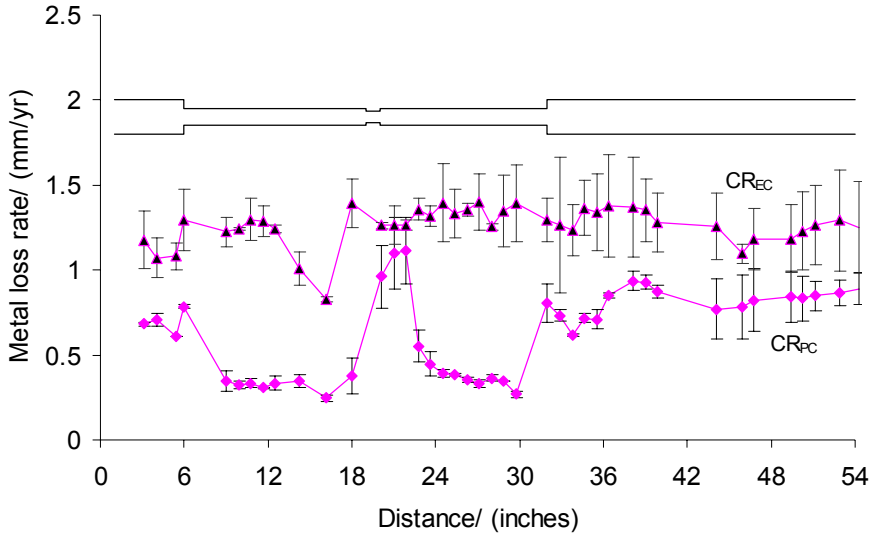

Figure 13. Comparison of pure corrosion (single phase flow, pH 4, PCO2 1.2bar, 24 hrs) and corrosion component in combined erosion-corrosion attack (2%wt sand slurry, pH 4, PCO2 1.2bar, 4 hrs, silica sand).

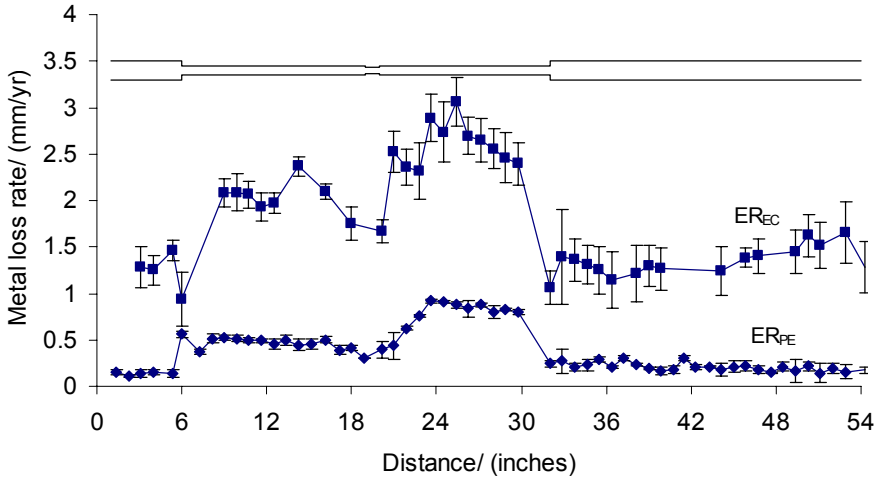

Figure 14. Comparison of pure erosion (2%wt sand slurry, pH 7, PN2 1.2bar, 4 hrs, silica sand) and erosion component in combined erosion-corrosion attack (2%wt sand slurry, pH 4, PCO2 1.2bar, 4 hrs, silica sand).

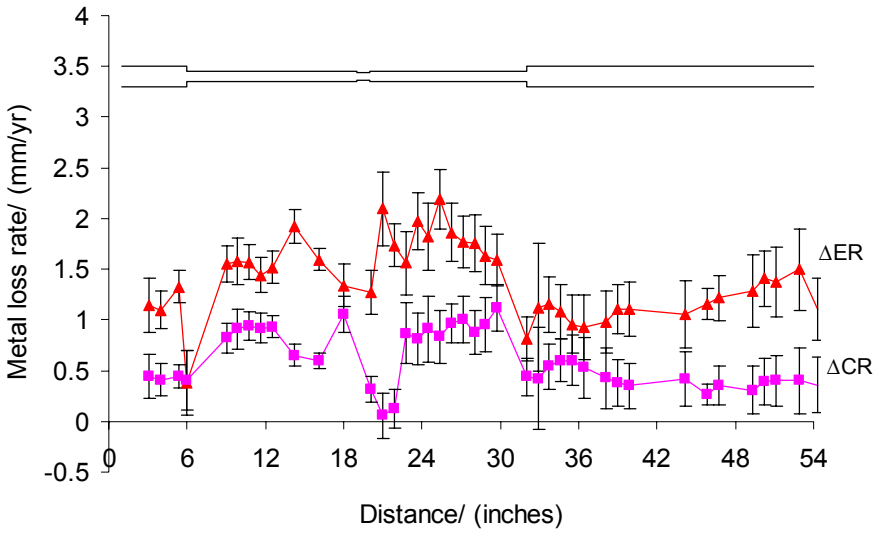

Figure 15. Increments in erosion and corrosion due to their interactions.

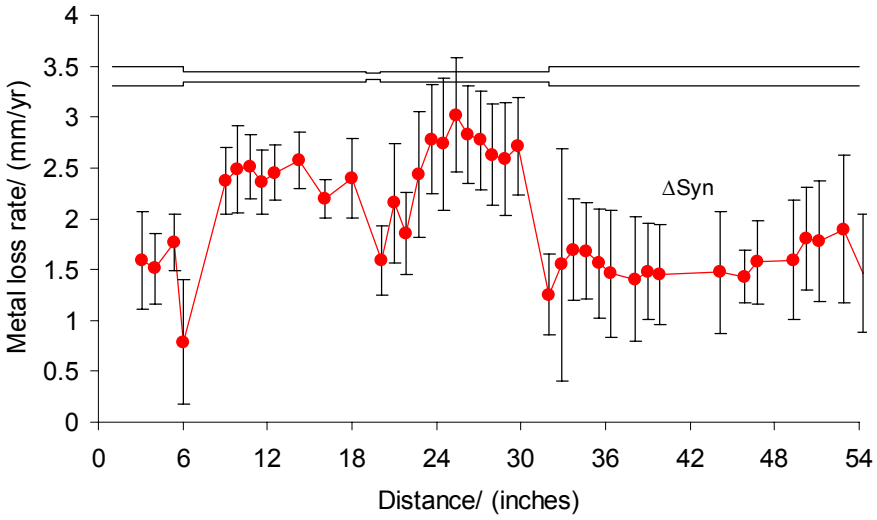

Figure 16. Net synergism across the flow disturbances.

(a)

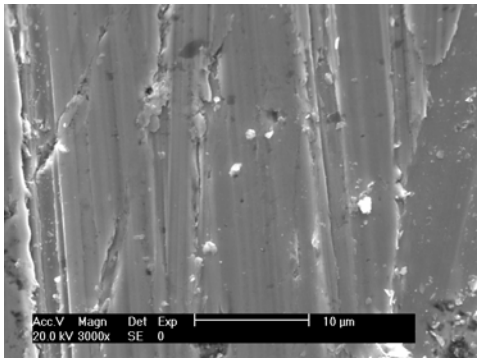

(b)

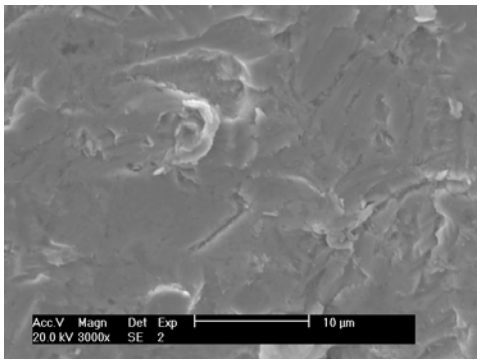

(c)

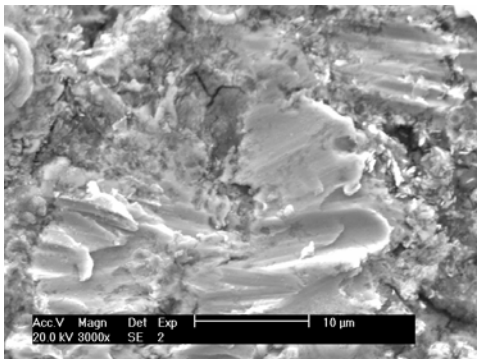

Figure 17. Appearance of the steel specimen surface before exposure (a), after exposure to pure erosion (b), and after exposure to erosion-corrosion (c).

CONCLUSIONS

1. A new, unique and simple test section has been designed that permits study of erosion-corrosion in realistic pipe flow conditions including disturbed flow geometries.
2. The approach allows the quantification of individual contributions by corrosion and erosion towards the total rate of attack. It also enables the separation of various types of synergism in erosion-corrosion.
3. In a combined erosion-corrosion process, corrosion and erosion enhance one another resulting in significant synergism.
4. Enhancement of erosion by corrosion is the dominant mechanism in the synergism under the conditions in this study where no corrosion films were present.

REFERENCES

1. Neville A., and Hodgkiess T., "Study of effect of liquid corrosivity in liquid-solid impingement on cast iron and austenitic stainless steel," BRITISH CORROSION JOURNAL, 1997, vol. 32, n 3, page no. 197

2. Salama M.M., "Influence of sand production on design and operations of piping systems," CORROSION 2000, paper no. 80

3. McLaury B.S., Shirazi S.A., Shadley J.R., Rybicki E.F., "Parameters affecting flow accelerated erosion and erosion-corrosion," CORROSION 1999, paper no. 120

4. Neville, A., Hodgkiess T., and Dallas J.T., "A study of the erosion-corrosion behavior of engineering steels for marine pumping applications," p 497, WEAR 186-187, 1995, page no. 497-507

5. Burstein G.T., Sasaki k., "Effect of impact angle on the erosion-corrosion of 304L stainless steel," WEAR 186-187, 1995, page no. 80-94

6. Zhou S., Stack M.M. and Newman R.C., "Characterization of synergistic effects between erosion and corrosion in an aqueous environment using electrochemical techniques," CORROSION SCIENCE 1996, vol. 52, n 12, page no. 934

7. Yugui Zheng, Zhiming Yao, Xiangyun Wei, Wei Ke, "The synergistic effect between erosion, corrosion in acidic slurry medium," WEAR 186-187, 1995, page no. 555-561

8. Madsen B.W., “Measurement of erosion-corrosion synergism with a slurry wear test apparatus,” WEAR OF MATERIALS 1987, Vol. 2, page no. 777-786

9. Hubner W., and Leitel E., “Peculiarities of erosion-corrosion processes,” TRIBOLOGY INTERNATIONAL 1996, Vol. 29, n 3, page no. 199

10. Wood R.J.K., and Hutton S.P., “The synergistic effect of erosion and corrosion: trends in published results,” WEAR 140, 1990, page 387-394

11. Watson S.W., Friedersdorf F.J., Madsen B.W., and Cramer S.D., “Methods of measuring wear-corrosion synergism,” WEAR 181-183, 1995, page no. 476-484

12. Lotz U., and Postlethwaite, J., “Erosion-corrosion in disturbed two phase liquid/particle Flow,” CORROSION SCIENCE 1990, Vol. 30, n 1, page no. 95

13. Blatt, W., Kohley T., Lotz U. and Heitz E., “The influence of hydrodynamics on erosion-corrosion in two-phase liquid-particle flow,” CORROSION SCIENCE 1989, Vol. 45, n 10, page no. 793

14. Nesic, S. and Postlethwaite, J., “Erosion in Disturbed Liquid/Particle Pipe Flow: Effects of Flow Geometry and Particle Surface Roughness,” p 850, CORROSION ENGINEERING 1993, Vol 49, n 10, page no.850

15. Kermani M. B. and Morshed A., “Carbon dioxide corrosion in oil and gas production-a compendium,” Corrosion 2003, Vol.59, No. 8, page no. 659

16. Nesic S., Postlethwaite J., and S. Olsen, “An electrochemical model for prediction of CO_2 corrosion,” CORROSION 1995, paper no. 131

17. Finnie I., “Some reflections on the past and future of erosion,” WEAR 186-187, 1995, page no. 1-10

18. Alan L.V., “Solid particle erosion and erosion-corrosion of materials,” ASM INTERNATIONAL, c 1995

19. Meng, H.C., and Ludema, K.C., “Wear models and predictive equations: their form and content,” WEAR 181-183, 1995, page no. 443-457

20. Postlethwaite J., “Effect of chromate inhibitor on the mechanical and electrochemical components of erosion-corrosion in aqueous slurries of sand,” CORROSION 1981, Vol. 37, n 1, page no. 1

21. Matsumura M., oka Y., Hiura H., and Yano M., “The role of passivating film in preventing slurry erosion-corrosion of austenitic stainless steel,” ISIJ Int. 1991, Vol. 31, n 2, page no. 168-176

22. Burstein G.T., Li Y., and Hutchings I.M., “The influence of corrosion on the erosion of aluminum by aqueous silica slurries,” WEAR 186-187, 1995, page no. 515-522

23. Neville A., Reyes M. and Xu H., “Examining corrosion effects and corrosion/erosion interactions on metallic materials in aqueous slurries,” TRIBOLOGY INTERNATIONAL 2002, vol. 35, page no. 643-650

24. Denny A. Jones, “Principles and prevention of corrosion,” Chapter 5, second edition, Prentice Hall, c1996

ACKNOWLEDGMENT

We would like to thank the technical staff at the Institute for Corrosion and Multiphase Technology at Ohio University, and particularly Mr. Al Schubert, Mr. Bruce Brown and Mr. John Goettge for their support and contribution in making this work a success. The contribution of a consortium of companies whose continuous financial support and technical guidance made this research at the Ohio University Institute for Corrosion and Multiphase Technology possible.